Theor Chem Acc (2006) 116: 462–471
DOI 10.1007/s00214-006-0082-8

REGULAR ARTICLE

B. Bories · S. Evangelisti · D. Maynau · T. Leininger

Two-body reduced density matrix reconstruction for Van der Waals systems

Received: 10 December 2004 / Accepted: 26 May 2005 / Published online: 8 March 2006

Abstract A method for the calculation of the electronic energy of a correlated system is presented. This approach is based on the reconstruction of the total two-body reduced density matrix by doing separate configurations interaction calculations on fragments. The method has been tested on Van der Waals systems and has been implemented by considering restrictive N-representability conditions. It is shown that the computational strategy presented in this work can describe with good accuracy weak dispersion interactions, and considerably lowers the size-consistency error of a classical configuration interaction calculation.

1 Introduction

The problem of accurate ab initio calculations is mainly due to their computational costs. By taking into account the correlation effects, the computational cost grows rapidly with the system size up to N^7 depending on the correlated method considered [1]. This fact has been the starting point of research works on N-scaling methods, that scale as a function of the system size. In particular, SCF, DFT, and single-reference (SR) correlated methods (like configuration interaction (CI), coupled cluster (CC), or perturbative approaches) have been implemented for a few years now into N-scaling algorithms [2–8]. On the other hand, with the exception of recent works of Carter et al. [1,7,8], little has been done in the field of N-scaling multi-reference methods. This important research framework is still largely unexplored.

Recently two independant works [9,10] on linear chain of hydrogens have been published. In these studies, a hydrogen chain is decomposed into a set of overlapping subsystems. The authors of both works used the formalism of the reduced density matrices (RDM) in order to calculate the two-body RDM (2-RDM) of the whole system. In this way, the total electronic energy can be retrieved, *without the need of a computation on the whole system*. These approaches use the fact that the two-body cumulant (2-CRDM), which represents the correlated part of the 2-RDM (in other words, the 2-CRDM is the part of the 2-RDM which can not be represented by a Grassmann product of the one-body RDM (1-RDM) [11]), presents local properties for non-metallic systems, and is additively separable [12]. Therefore, since the 2-CRDM is for its major part restrained in a local region, the total 2-RDM can be approximated by the sum of the local contributions of overlapping subsystems in the 2-CRDM, the rest of the 2-RDM being estimated by the Grassmann product of the corresponding elements of the 1-RDM. For this reason, methods based on 2-CRDM have in principle a N-scaling behavior, provided one works with local orbitals.

In this paper, the formalism related to the local property of the 2-CRDM is presented. It is important to note that the present method is based on wave function calculations on each subsystem, which permit reconstruction of the total 2-RDM of the system under interest and then to retrieve the average values of any bielectronic operator (e.g., the electronic Hamiltonian). In this study, only single and double CI (SD-CI) calculations on each subsystem were done, while keeping the rest of the molecule frozen at the HF level. This work focuses on the accurate description of dispersion effects, which are the major source of interaction in Van der Waals systems. As test cases, linear chains of Helium atoms and the He [4] cluster have been considered.

This article is organized as follows: In Sect. 2, the general formalism is presented. The problems related to the N-representability of the 2-RDM are discussed in Sect. 2.1. Some powerful necessary (but non sufficient) N-representability conditions, the D, Q, and G conditions [13] are presented. In the next subsection, the RDM formalism and the N-representability problem are briefly recalled [13]. Then, in Sect. 2.3, the general framework of our approach is presented. In Sect. 3, the application to Helium clusters is reported. In particular, linear chains of six atoms of Helium with a small

---

B. Bories (✉) · S. Evangelisti · D. Maynau · T. Leininger
Laboratoire de Physique Quantique, UMR 5626,
Université Toulouse III, 118, route de Narbonne,
31062 Toulouse, France
E-mail: juantofr@yahoo.com
Tel.: 33-561-556361

basis set have been considered firstly (Sect. 3.1), followed by an application of the method to the same linear chain and the Helium cluster [4] in a larger basis set (Sect. 3.2).

2 General formalism

2.1 Reduced density matrix formalism

A summary of the RDM formalism is given in this section, where the most important properties of these objects are recalled. Since the present density matrix reconstruction method implies only the 1-RDM and 2-RDM, we focus on these two objects only.

In an orthonormal basis of spinorbitals and with $|\Psi\rangle$ eigenfunction of S_z, the 1-RDM is defined in second quantification by:

$$^{1}\Gamma^{i\sigma}_{j\sigma} = \langle\Psi|\, a^{+}_{i\sigma} a_{j\sigma}\, |\Psi\rangle \tag{1}$$

and the 2-RDM by:

$$^{2}\Gamma^{i\sigma j\sigma'}_{k\sigma l\sigma'} = \frac{1}{2}\,\langle\Psi|\, a^{+}_{i\sigma} a^{+}_{j\sigma'} a_{l\sigma'}\, a_{k\sigma}\, |\Psi\rangle\,, \tag{2}$$

where σ and σ' represent the spin labels and $\{i,\ j,\ k,\ l\}$ the spatial orbitals labels.

The total electronic energy can be expressed as a function of the 1-RDM and the 2-RDM:

$$E = \sum_{i,j}^{\sigma,\sigma'} {}^{1}\Gamma^{i\sigma}_{j\sigma}\, h_{i\sigma j\sigma} + \sum_{i,j,k,l}^{\sigma,\sigma'} {}^{2}\Gamma^{i\sigma j\sigma'}_{k\sigma l\sigma'}\, \langle i_\sigma\, j_{\sigma'}|k_\sigma l_{\sigma'}\rangle \tag{3}$$

with $h_{i\sigma j\sigma} = \int i^*(x_1)\, h(x_{1)}\; j(x_1)\, \mathrm{d}x_1$, $\langle i_\sigma\, j_{\sigma'}|k_\sigma l_{\sigma'}\rangle = \int\int i^*(x_1)\; j^*(x_2)\, r_{12}^{-1}\, k(x_1)\, l(x_2)\, \mathrm{d}x_1\, \mathrm{d}x_2, x_1,\ x_2$ are the coordinates of the electrons 1 and 2 upon the spin and orbital spaces.

The 2-RDM has several interesting properties [14–19]:

1. it is symmetric under a permutation of a particle
$$^{2}\Gamma^{i\sigma j\sigma'}_{k\sigma l\sigma'} = {}^{2}\Gamma^{j\sigma i\sigma'}_{l\sigma k\sigma'}, \tag{4}$$
2. it is antisymmetric under a permutation of a spinorbital
$$^{2}\Gamma^{i\sigma j\sigma'}_{k\sigma l\sigma'} = -{}^{2}\Gamma^{j\sigma i\sigma'}_{k\sigma l\sigma'}, \tag{5}$$
3. it is hermitian
$$^{2}\Gamma^{i\sigma j\sigma'}_{k\sigma l\sigma'} = ({}^{2}\Gamma^{k\sigma l\sigma'}_{i\sigma j\sigma'})^{*}. \tag{6}$$

In addition to these properties, implied by the creation and annihilation operator formalism used in the definition, RDM must be "N-representable," i.e., obtained from a N-electron wave function. Unfortunately, this N-representability problem is still unresolved for the 2-RDM [14,20–22]. On the contrary, as far as ensemble 1-RDMs are concerned, sufficient and necessary conditions are known for ensemble 1-RDMs [14] and are given by:

$$0 \le n_p \le 1, \tag{7}$$

where n_p are the eigenvalues of the 1-RDM.

Further conditions can be imposed if the wave function is eigenfunction of the number operator (it is the case of the eigenfunctions of the Hamiltonian in non-relativistic quantum mechanics). These are the "trace conditions" for the 1-RDM and the 2-RDM:

$$\mathrm{Tr}({}^{1}\Gamma) = N, \tag{8}$$

$$\mathrm{Tr}({}^{2}\Gamma) = \frac{N(N-1)}{2}, \tag{9}$$

where N is the number of electrons.

Even though the N-representability conditions known for the 2-RDM are only necessary, some of them are very restrictive as Mazziotti [21] or Nakata showed [22] in the frame of the Contracted Schrödinger Equation formalism. The conditions given below must be considered in addition to the Eqs. (4), (5), (6), (7), and (8): the conditions known as D, Q, and G conditions are formulated by using the two-electron density matrix (D), the two-hole density matrix (Q) and the electron-hole density matrix (G) [20–22]. These matrices must be all non-negative (non-negativity of a matrix means that all its eigenvalues are greater or equal to zero).This is because they can be expressed as metric matrices which can generate any mean value of a bielectronic operator [15,23]. These non-negativity conditions can be reformulated as:

$$^{2}D^{i\sigma j\sigma'}_{k\sigma l\sigma'} = \langle\Psi|\, a^{+}_{i\sigma} a^{+}_{j\sigma'} a_{l\sigma'}\, a_{k\sigma}\, |\Psi\rangle = 2\,{}^{2}\Gamma^{i\sigma j\sigma'}_{k\sigma l\sigma'}, \tag{10}$$

$$\begin{aligned} {}^{2}Q^{i\sigma j\sigma'}_{k\sigma l\sigma'} &= \frac{1}{2}\,\langle\Psi|\, a_{i\sigma} a_{j\sigma'} a^{+}_{l\sigma'} a^{+}_{k\sigma}\, |\Psi\rangle \\ &= {}^{2}D^{k\sigma l\sigma'}_{i\sigma j\sigma'} - \delta^{l}_{j}\, {}^{1}\Gamma^{k\sigma}_{i\sigma} - \delta^{k}_{i}\, {}^{1}\Gamma^{l\sigma'}_{j\sigma'} \\ &\quad +\delta^{l}_{j}\, \delta^{k}_{i} + \delta^{l}_{j}\, \delta^{k}_{i} \\ &\quad +\delta^{\sigma'}_{\sigma}\, (\delta^{i\sigma}_{l\sigma'}\, {}^{1}\Gamma^{j\sigma}_{k\sigma} + \delta^{j\sigma}_{k\sigma}\, {}^{1}\Gamma^{i\sigma}_{l\sigma} - \delta^{j\sigma}_{k\sigma}\delta^{i\sigma}_{l\sigma}), \end{aligned} \tag{11}$$

$$\begin{aligned} {}^{2}G^{i\sigma j\sigma'}_{k\sigma l\sigma'} &= \frac{1}{2}\,\langle\Psi|\, a^{+}_{i\sigma} a_{j\sigma'} a^{+}_{l\sigma'}\, a_{k\sigma}\, |\Psi\rangle \\ &= -{}^{2}D^{i\sigma l\sigma'}_{k\sigma j\sigma'} + \delta^{l}_{j}\, {}^{1}\Gamma^{i\sigma}_{j\sigma}. \end{aligned} \tag{12}$$

In previous works [24,25], by imposing the D, Q, and G conditions, it was possible to obtain quasi N-representable 2-RDM. Indeed, if these three conditions were not verified, the total electronic energy could be even 100% lower than the FCI one for the cases considered. On the other hand, when these conditions were satisfied, the total electronic energy was at most 5% lower than the FCI one. As a result of these previous works [24,25], the D, Q, and G conditions (in addition to the conditions (4), (5), and (6)) were used to check the quality of the reconstructed 2-RDM.

In the present work, the main interest of the 2-RDM is given by its cumulant expansion. The cumulant expansion of the 2-RDM can be defined as [26]:

$$^{2}\Gamma^{ij}_{kl} ={}^{1}\Gamma^{i}_{k} \times {}^{1}\Gamma^{j}_{l} - {}^{1}\Gamma^{i}_{l} \times {}^{1}\Gamma^{j}_{k} + {}^{2}\Lambda^{ij}_{kl}, \tag{13}$$

where $^{2}\Lambda^{ij}_{kl}$ represents the 2-CRDM which is the two-body correlation part of the 2-RDM [27,28]. The 2-CRDM vanishes when the two particles are statistically independent.

The two-body correlation part of the 2-RDM is contained in a small volume compared to the size of the problem studied. This property has been studied in a previous work [10] with linear chains of hydrogen atoms where the long-range correlation effects, meaning non-negligible values of the 2-CRDM at long distances, only occurred for metallic cases. This simple observation is the basic idea of the present two-body reduced density matrix reconstruction method.

It must be noticed that the 2-CRDM is extensive, contrary to the 2-RDM [28–30]. (A quantity is said to be extensive when it is additively separable: the total quantity of a system made of two non-interacting subsystems is equal to the sum of the individual quantities of each subsystem.) For this reason, this cumulant expansion can be advantageously used to express the electronic energy of two weak interacting subsystems.

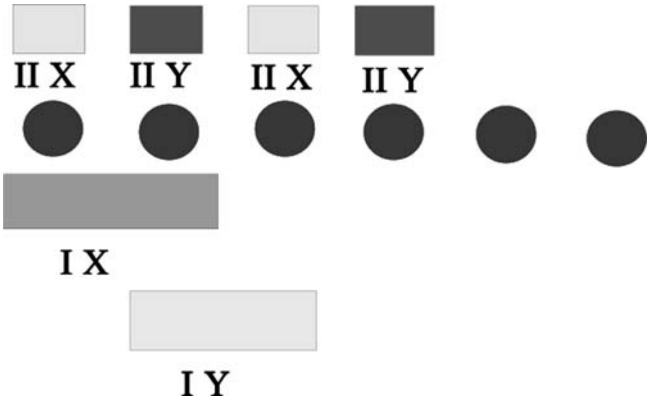

Fig. 1 Two types of fragments (I and II) used in the 2-RDM-R method. We have represented two fragments of type I (I X and I Y) and two of type II (II X and II Y)

2.2 The two-body reduced density matrix reconstruction method (2-RDM-R)

The main idea of the 2-RDM-R is based on the expression of the total electronic energy (3) and the cumulant expansion of the 2-RDM (13).

It has been shown that for an insulator, the 1-RDM decays as $e^{-\alpha r}$, r being the distance between two spinorbitals of an element of the 1-RDM, ${}^1D^{i_\sigma}_{j_{\sigma'}}$ and α is a function of the HOMO–LUMO gap [31]. This property has been used by Kohn [32] to propose a linear-scaling procedure to obtain the total 1-RDM of a system treated as a sum of subsystems. Indeed, the linear-scaling procedures using the density matrix formalism deal only with the one-body density matrix. Nevertheless, with the cumulant expansion, we can propose a low computational cost procedure involving also the 2-RDM.

In the present work, SD-CI calculations are performed on fragments of the system under study, while keeping the remaining parts of the system frozen at the SCF level. From these calculations, the 2-RDM$_{\text{sub}}$ and 1-RDM$_{\text{sub}}$ for each fragment are extracted, and the total 1-RDM and 2-RDM are then reconstructed. Thus, for each fragment, atom-centered orbitals belonging to each subsystem are defined. As Van der Waals systems are dispersive ones, one must be able to calculate the dispersive energy, which decreases as r^{-6} [33], with a good accuracy. Molecular fragments (fragments of type I) are defined as in our previous work [10]. A second type of molecular fragments is needed for the calculation of the dispersive energy, i.e., non-contiguous fragments (fragments of type II). The two types of fragments in the case of a linear chain He$_6$ are shown in Fig. 1. Fragments of type I are composed of two adjacent atoms, whereas fragments of type II involve two atoms that are separated by at least one atom, and are required for the description of long-range interactions. For example, one fragment of type II called IIA includes the first and third atoms in Fig. 1, another one called IIB includes the second and fourth atoms. It is necessary that the two types of fragments contain the same number of electrons and hence the same number of occupied orbitals to avoid a costly renormalization process of the elements of the 2-RDM and 1-RDM obtained during the reconstruction process. This has been made in order to clear the algorithm. Moreover, we decided to consider only two-electron fragments, in order to prove that the method could supply accurate results for Van der Waals systems by using small fragments only, and implying therefore a low computational cost. However, in the case of large systems with long-range interactions, it would be possible to use larger fragments (under the condition that the size of the fragment remains small in comparison to the whole system).

The obtention of the total 1-RDM and 2-RDM depends on the type of fragment used. For fragments of type I labeled $\{A, B, \ldots, I\}$, the total 1-RDM can be expressed as

$$\text{if } (i,j) \in A, \quad {}^1\Gamma^{i\sigma}_{j\sigma} = {}^1\Gamma^{i\sigma}_{j\sigma_{\text{sub A}}} \tag{14}$$

and

$$\text{if} i \in A \text{ and } j \notin A, \quad {}^1\Gamma^{i\sigma}_{j\sigma} = 0 \tag{15}$$

where the subscript sub means that a given element has been obtained from a calculation on the considered fragment.

The elements of the 2-RDM are then obtained from the cumulant expansion (13):

$$\text{if } (i,j,k,l) \in A, \quad {}^2\Gamma^{i\sigma,j\sigma'}_{k\sigma,l\sigma'} = {}^2\Gamma^{i\sigma,j\sigma'}_{k\sigma,l\sigma'_{\text{sub A}}} \tag{16}$$

$$\text{if } (i,k) \in A \text{ and } (j,l) \in B, \quad {}^2\Gamma^{i\sigma,j\sigma'}_{k\sigma,l\sigma'} = {}^1\Gamma^{i\sigma}_{k\sigma'_{\text{sub A}}}\,{}^1\Gamma^{j\sigma}_{l\sigma'_{\text{sub B}}} \tag{17}$$

$$\text{if } (i,l) \in A \text{ and } (j,k) \in B, \quad {}^2\Gamma^{i\sigma,j\sigma'}_{k\sigma,l\sigma'} = -{}^1\Gamma^{i\sigma}_{l\sigma'_{\text{sub A}}}\,{}^1\Gamma^{j\sigma}_{k\sigma'_{\text{sub B}}} \tag{18}$$

Fragments of type II need to be considered to calculate some elements of the 2-RDM that cannot be satisfactorily approximated by a product of the corresponding elements of the 1-RDM. Concerning the elements of the 1-RDM, these fragments represent non-neighbor atoms and thus the only non-negligible elements of the 1-RDM which can be

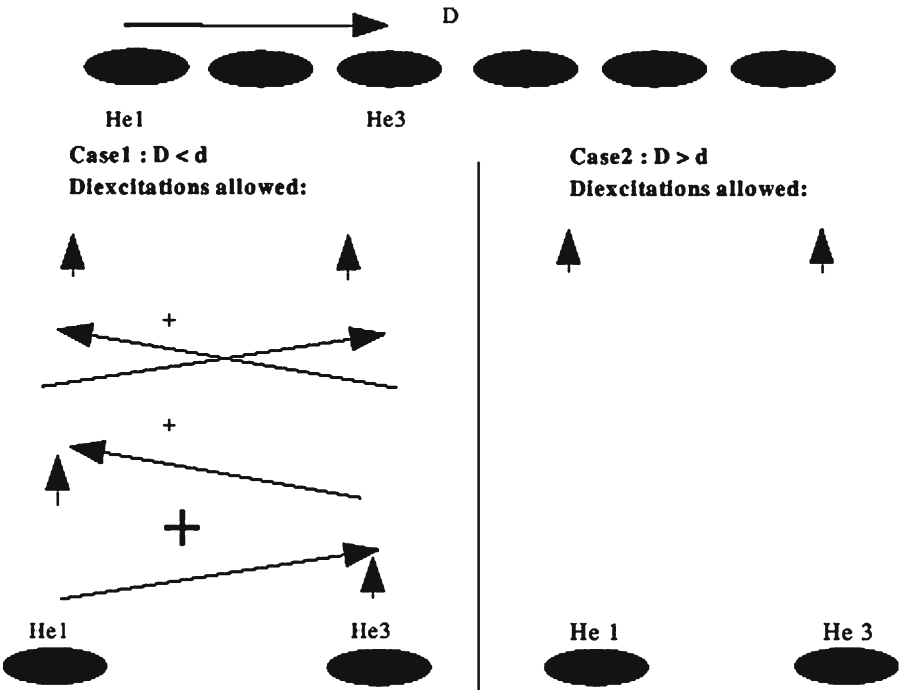

Fig. 2 The principle of the "Antisymmetrized approximation" is described in terms of diexcitations considered as a function of the distance D separating two non-neighbor atoms He1 and He3 (He1 and He3 constituting a whole fragment of type II defined in Fig. 1). d is the cut-off radius beyond of which the approximation is done. This principle is only used for fragments of type II (see Fig. 1)

extracted from such fragments are best approximated by calculations over fragments of type I.

To treat type II fragments, the "antisymmetrized approximation" [2] is introduced by defining a cut-off radius d. This approximation consists in neglecting ionic forms and taking only into account neutral forms which leads to increased computational savings. A graphic representation of this approximation is illustrated in Fig. 2. Thus, to summarize the calculations on fragments of type II, labeled $\{\alpha, \beta, \kappa \ldots\}$, one has:

if $(i, j, k, l) \in \alpha$ and $(i, j, k, l) \notin A$ and $[ijkl] < d$

$${}^2\Gamma^{i\sigma,j\sigma'}_{k\sigma,l\sigma'} = {}^2\Gamma^{i\sigma,j\sigma'}_{k\sigma,l\sigma'_{\mathrm{sub}\alpha}}, \tag{19}$$

if $(i, j, k, l) \in \alpha$ and $(i, k) \in A$ and $(j, l) \in B$ and $[ijkl] > d$,

$${}^2\Gamma^{i\sigma,j\sigma'}_{k\sigma,l\sigma'} = {}^2\Gamma^{i\sigma,j\sigma'}_{k\sigma,l\sigma'_{\mathrm{sub}\alpha}} \tag{20}$$

For all the other cases, Eqs. (17), (18), and (19) have been used.

The total electronic energy can then be expressed in terms of the reconstructed 1-RDM and 2-RDM (3). Note that the mean value of any observable C [13] which can be expressed as a bielectronic operator can be deduced from the reconstructed 2-RDM:

$$\langle C \rangle = \mathrm{Tr}({}^2\Gamma\, C). \tag{21}$$

Although the formalism appears to be quite straightforward, one has to choose with caution the fragments and check carefully some conditions that the reconstructed 2-RDM and 1-RDM must fulfill. The N-representability conditions are well suited for this task as will be shown in Sect. 3.2 for the test case He_6.

This antisymmetrized approximation has been previously proposed by Lee *et al.* [34] in an truncated ansatz of MP2. These authors considered double excitations implying three centers where one excitation involved one center and the other one two centers separated by a distance smaller than a predefined cut-off radius.

2.3 The EPV terms implied by the fragmentation of the diexcitations

The main reason is a size-extensivity ($|\Psi_{\mathrm{total}}\rangle = |\Psi_A\rangle \times |\Psi_B\rangle$, where A and B are non-interacting subsystems) error when we make successive SDCI calculations on each fragment. Indeed, we allowed forbidden diexcitations due to the separability of diexcitations introduced by the 2-RDM reconstruction method.

In the case of a system composed of two non-interacting subsystems, A and B, one has

$$C^{r_A s_A}_{i_A j_A} \otimes C^{t_B u_B}_{k_B l_B} = C^{r_A s_A}_{i_A j_A}\, C^{t_B u_B}_{k_B l_B}, \tag{22}$$

where the coefficients C are the coefficients of the diexcitations from CI calculations.

Here $(i_A; j_A)$, $(k_B; l_B)$ *and* $(r_A; s_A)$ $(t_B; u_B)$ represent occupied and virtual orbitals belonging to fragments A and B, respectively. $\otimes$ represents the normal product and contains the ordinary product as well as all the products generated by all the possible permutations between the eight orbitals considered.

In the case of a complete system, the wave function can be written using the intermediate normalization scheme:

$$|\Psi\rangle = |\Phi_0\rangle + \sum C_{ij}^{rs} a_r^{+} a_s^{+} a_j\, a_i\ |\Phi_0\rangle\ + \cdots . \tag{23}$$

By performing a calculation on each fragment, it is possible to express the SD-CI equations as:

$$E = E_0 + \sum C_{ij}^{rs}\ \langle ij|rs\rangle\ , \tag{24}$$

$$\begin{aligned}(\langle H\rangle_{kl}^{tu} - E_0)\, C_{kl}^{tu}\ \langle kl|tu\rangle = {} & \sum_{ijrs} C_{ij}^{rs}\left\langle \Phi_{kl}^{tu}\right| H \left|\Phi_{ij}^{rs}\right\rangle \\ & + \sum_{ijrs} C_{ijkl}^{rstu}\left\langle \Phi_{kl}^{tu}\right| H \left|\Phi_{ijkl}^{rstu}\right\rangle ,\end{aligned} \tag{25}$$

with $\langle H\rangle_{kl}^{tu} = \left\langle \Psi\, |H|\, \Phi_{kl}^{tu}\right\rangle$ and $\Phi_{kl}^{tu} = a_t^{+} a_u^{+} a_l\, a_k\ |\Phi_0\rangle$.

By performing separate calculations on each fragment, one includes diexcitations that are not allowed in SD-CI calculations on the whole system. This fact can easily be seen by considering the EPV terms [35] related to four orbitals (k, l, t, u) where (k, l) are occupied and (t, u) virtual orbitals.

$$\mathrm{EPV}\binom{tu}{kl} = \sum C_{ij}^{rs}\ \langle ij|rs\rangle\ , \tag{26}$$

where at least one of the four orbitals (i, j, r, s) corresponds to one orbital of the set (k, l, t, u). The EPV terms can be seen as disconnected diagrams between two fragments but with at least one common orbital.

The SD-CI equations can then be extended as:

$$\begin{aligned}&(\langle H\rangle_{kl}^{tu} - E_0 - \mathrm{EPV}\tbinom{tu}{kl})\, C_{kl}^{tu}\ \langle kl|tu\rangle \\ &\quad = \sum C_{ij}^{rs}\left\langle \Phi_{kl}^{tu}\right| H \left|\Phi_{ij}^{rs}\right\rangle + \sum C_{ijkl}^{rstu}\left\langle \Phi_{kl}^{tu}\right| H \left|\Phi_{ijkl}^{rstu}\right\rangle .\end{aligned} \tag{27}$$

Solving this equation will avoid taking into account the forbidden diexcitations. By considering the EPV terms in SD-CI equations, it is possible to include the repulsive dynamical-correlation effects between electrons, a major effect at short distances. This implies that, the EPV terms being neglected, the reconstructed 2-RDM is not strictly N-representable, and the total electronic energy is lower as the exact one. A solution to this drawback of the method could consist in selecting diexcitations when doing calculations on each fragment in order to take into account the EPVs, although this will not totally solve the problem of the size-extensivity of the 2-RDM-R method.

3 Application to Helium clusters

In this section, the method proposed above is illustrated through an application to the computation of the dispersion energy of Helium clusters.

3.1 Computational details

A linear chain of Helium atoms, which is a Van der Waals system characterized by pure dispersion bielectronic interactions, was considered. In a first step, a small basis set (ANO-l 2s) [14] was used in order to check all the desired N-representability conditions and compare the reconstructed 2-RDM with the FCI one although this basis set does not permit a good description of dispersion effects. The interatomic distance was varied from 2.5 to 6.0 Å. The localization was done with the computer suite of programmes of Maynau *et al.* [36] to obtain atom-centered orbitals. Projecting the local guess orbitals on the SCF delocalized ones to obtain local orbitals of Hartree-Fock quality gave better results. To check that the method effectively lowers the size-consistency error of SD-CI calculation, calculations were done on each fragment with the CASDI [37] program, keeping the rest of the system frozen at the Hartree-Fock level. The new code gathers then the elements of the 1-RDM$_{\mathrm{sub}}$ and the 2-RDM$_{\mathrm{sub}}$ to calculate the total 1-RDM and 2-RDM according to the 2-RDM-R formalism presented in the previous section. Moreover, the algorithm has been implemented to allow direct calculations of the elements of the 1-RDM and the 2-RDM in order to avoid storage problems.

3.2 Results of the study of the linear chain He$_6$ in a small basis set

We have checked the N-representability conditions given by equations D, Q, G, and trace conditions for the 2-RDM (9), (10), (11), and (12). The reconstructed 2-RDM automatically fulfils the hermiticity and symmetry/antisymmetry conditions with respect to a permutation of a particle or a spinorbital, respectively (4), (5), and (6). The D, Q, and G conditions imply the diagonalization of the corresponding matrices and the positivity of their eigenvalues.

Thus, these matrices were diagonalised in the set of the geminals g_μ(functions of two particles) expressed as antisymmetrised products of the orbitals $\{\varphi_i\}$:

$$g_\mu(r_1; r_2) = \frac{1}{\sqrt{2}}(\varphi_i(r_1)\varphi_k(r_2) - \varphi_i(r_2)\varphi_k(r_1)). \tag{28}$$

In this geminal basis, one has the relation:

$${}^2\Gamma_{\mu,\nu} = 2\,{}^2\Gamma_{k,l}^{i,j}. \tag{29}$$

Moreover, the 2-RDM can be considered as a 2 × 2 blocks matrix:

$${}^2\Gamma = \left\| \begin{matrix} {}^2\Gamma^{\alpha,\alpha} & {}^2\Gamma^{\alpha,\beta} \\ {}^2\Gamma^{\beta,\alpha} & {}^2\Gamma^{\beta,\beta} \end{matrix} \right\| . \tag{30}$$

For singlet configurations,

$${}^2\Gamma^{\alpha,\alpha} = {}^2\Gamma^{\beta,\beta} \quad \text{and} \quad {}^2\Gamma^{\beta,\alpha} = {}^2\Gamma^{\alpha,\beta}. \tag{31}$$

The blocks ${}^2\Gamma^{\alpha,\alpha}$ and ${}^2\Gamma^{\beta,\alpha}$ were considered separately in order to check the D, Q, and G conditions.

For the 1-RDM, Eqs. (7), and (8) were also checked.

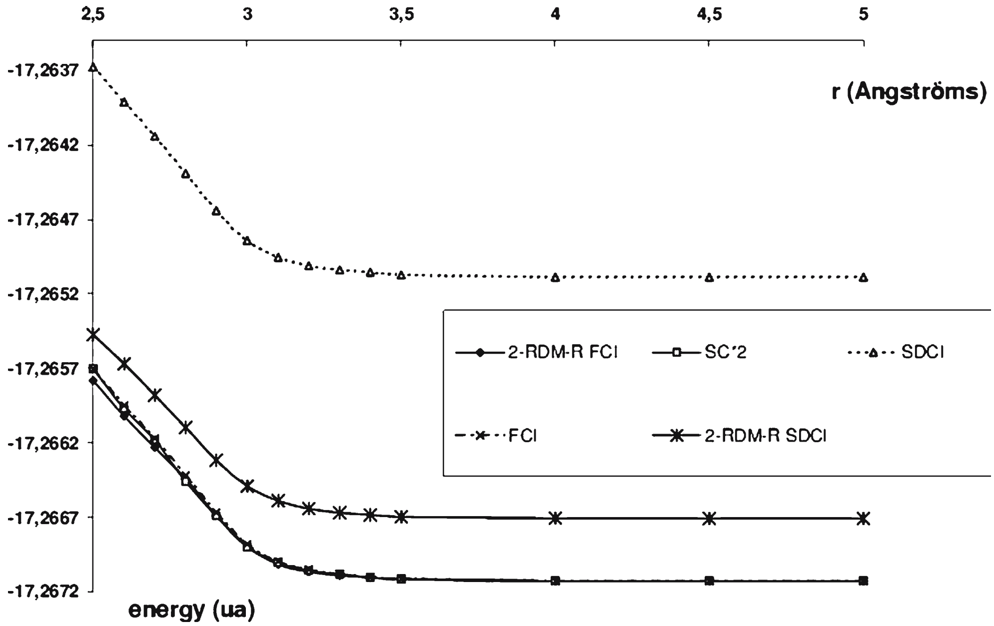

Fig. 3 Total electronic energies for a linear chain of six Helium atoms in the (ANO-l, 2s) basis set for the 2-RDM-R^{FCI}, 2-RDM-R^{SDCI}, SDCI, FCI, and SC**2 methods as a function of the interatomic distance r

Two different ways to improve the 2-RDM-R method and the fragmentation view of the system were investigated.

First, the validity of the antisymmetrized approximation was explored to determine the best cut-off radius leading to both a non-negligible computational saving for large systems and high enough accuracy.

In the second step, some excitations from occupied orbitals belonging to a fragment A to the virtuals belonging to the neighbour fragment B were allowed for the calculation done on the fragment A.

In the case of an SDCI calculation on fragment A, the wave function may be written as:

$$|\Psi\rangle = |\Psi_{\text{mono}}\rangle + |\Psi_{\text{di}}\rangle \tag{32}$$

with

$$|\Psi_{\text{mono}}\rangle = \sum C_{i\sigma}^{a\sigma}\left|\Psi_{i\sigma}^{a\sigma}\right\rangle + \sum C_{i\sigma}^{r\sigma}\left|\Psi_{i\sigma}^{r\sigma}\right\rangle \tag{33}$$

and

$$\begin{aligned} |\Psi_{\text{di}}\rangle = {} & \sum C_{i\sigma j\sigma'}^{a\sigma b\sigma'}\left|\Psi_{i\sigma j\sigma'}^{a\sigma b\sigma'}\right\rangle + \sum C_{i\sigma j\sigma'}^{r\sigma b\sigma'}\left|\Psi_{i\sigma j\sigma'}^{r\sigma b\sigma'}\right\rangle \\ & + \sum C_{i\sigma j\sigma'}^{a\sigma s\sigma'}\left|\Psi_{i\sigma j\sigma'}^{a\sigma s\sigma'}\right\rangle + \sum C_{i\sigma j\sigma'}^{r\sigma s\sigma'}\left|\Psi_{i\sigma j\sigma'}^{r\sigma s\sigma'}\right\rangle \end{aligned} \tag{34}$$

with $(i, j, a, b) \in A$ and $(r, s) \in \{B, C, \ldots\},\{B, C, \ldots\}$ being the set of neighbor fragments of A.

Then, only the elements of the 1-RDM and 2-RDM corresponding to spinorbitals belonging to A were extracted from this calculation.

The subsections below present the results obtained considering the antisymmetrized approximation and the extended excitation spaces. The N-representability conditions are tested in order to show the improvement in the reconstruction of the 2-RDM.

3.2.1 Validity of the antisymmetrized approximation

The energy errors for the antisymmetrized approximation for values of the cut-off radius d going from 2.5 to 10 Å with the 2-RDM-R^{SDCI} method were calculated. For $d = 4.0$ Å, the method leads to computational efficiency without loss of accuracy since the energies obtained differ only by 2×10^{-6} hartree from results obtained without this approximation. This value is in good concordance with that of Pulay and Saebo for the LMP2 method [2]. Moreover, this approximation does not affect the N-representability conditions fulfilled by our reconstructed 2-RDM and 1-RDM.

3.2.2 Comparison of the results of each method

All the results presented here used the antisymmetrized approximation with a cut-off radius of 4 Å and SDCI (or FCI) calculations on each fragment allowing excitations to virtual orbitals belonging to the neighbor fragments. The results of the 2-RDM-R^{SDCI} and 2-RDM-R^{FCI} obtained by SDCI and FCI calculations, respectively, on each fragment, are compared with the SD-CI, the FCI and the SC*2 methods (see Figs. 3 and 4). The SC*2 method [39] is a size-consistency correction method for an SD-CI calculation. The 2-RDM-R^{FCI} results were added to show this.

With the small basis set used the system is found to be repulsive (the bond length at a very high level of calculation of He_2 is 3.2 Å [38]). The results are encouraging in the sense that the 2-RDM-R considerably lowers the size-consistency error of a classical SDCI calculation and implies a lower computational cost than other corrective methods proposed in previous works [38,40,41]. At very short distances (2.5 Å, where the results are the poorest) the error is

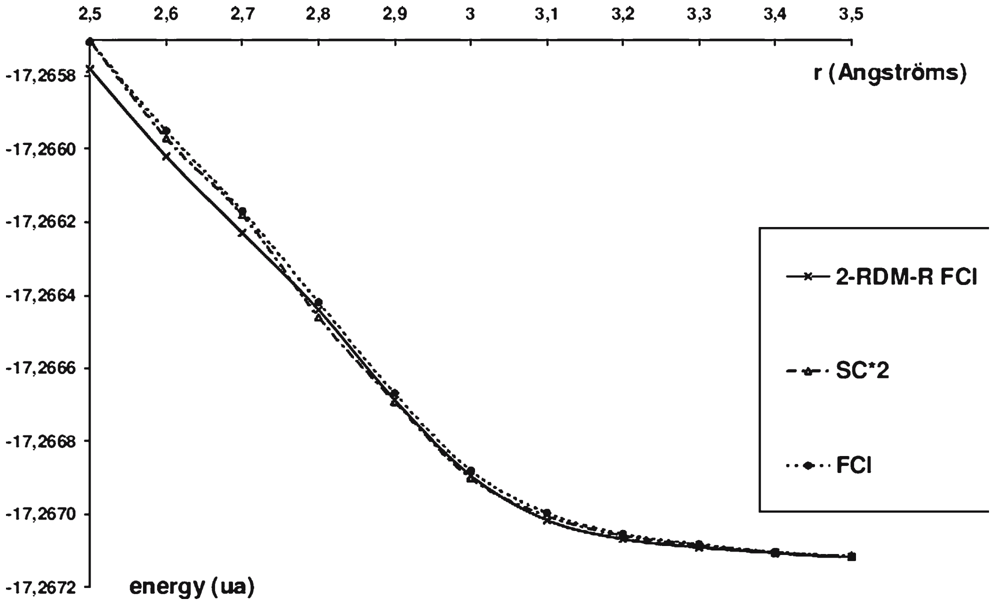

Fig. 4 Zoom of Fig. 3 for an interatomic distance $r(r \in [2.5; 3.5])$ Angströms and for the SC**2, FCI and 2-RDM-R$^{\mathrm{FCI}}$ methods

only of 2.7115×10^{-4}hartrees for the 2-RDM-R$^{\mathrm{SDCI}}$ method whereas it amounts to 2.0293×10^{-3} hartrees for a classical SDCI calculation. Moreover, the computational cost of the 2-RDM-R$^{\mathrm{SDCI}}$ method grows as $N_{\mathrm{sub}\,I+\mathrm{sub}\,II} * (n/N_{\mathrm{sub}I})^2$ $(N/N_{\mathrm{sub}I})^4$ whereas the computational cost of the SDCI method grows as n^2N^4 [1], where n is the total number of occupied orbitals, N the total number of basis functions, $N_{\mathrm{sub}I}$ the number of fragments of type I and $N_{\mathrm{sub}I+\mathrm{sub}II}$ the total number of fragments (type I and type II) . Actually, the accuracy of the 2-RDM-R$^{\mathrm{SDCI}}$ method is not constant versus the FCI results. the method being more reliable for distances larger than the equilibrium one.

Table 1 The evolution of the N-representability conditions obtained at variable distances

rÅ	Conditions	α, α Block	α, β Block
2.5			
	D matrix	20 (17)	18 (16)
	Q matrix	20 (17)	18 (16)
	G matrix	0 (0)	0 (0)
	Trace error	3.503 E − 5	3.580 E − 5
3.2			
	D matrix	1 (1)	0 (1)
	Q matrix	1 (1)	0 (1)
	G matrix	0 (0)	0 (0)
	Trace error	3.304 E − 6	3.371 E − 6
6.0			
	D matrix	1 (0)	0 (0)
	Q matrix	1 (0)	0 (0)
	G matrix	1 (0)	0 (0)
	Trace error	1.96 E − 11	2.7 E − 11

Table 2 The N-representability conditions at an interatomic distance of 2.57 Å

	α, α Block	α, β Block
D matrix	20 (1)	10 (0)
Q matrix	20 (1)	10 (0)
G matrix	1 (1)	0 (0)
Trace error	2.080 E − 6	1.082 E − 6

3.2.3 *Effects of the choice of the virtual space for each fragment*

Not allowing electrons to go to virtual orbitals belonging to neighbor fragments, the 2-RDM-R$^{\mathrm{FCI}}$ electronic energy for short distances is lower than the FCI one, which proves that the reconstructed 2-RDM does not fulfill the known N-representability conditions. This problem occurs also in density matrix minimisation method [25] or in the Contracted Schrödinger Equation [24]. We have represented in Table 1 the evolution of the N-representability conditions fulfilled by the reconstructed 2-RDM obtained at a distance of 2.5, 3.2, and 6.0 Å for a virtual space limited to the fragment itself (1 to 1 excitation space) for the 2-RDM-R$^{\mathrm{FCI}}$ and the 2-RDM-R$^{\mathrm{SDCI}}$ methods. Only negative eigenvalues of the D, Q, and G matrices smaller than -10^{-6} were considered.

In Table 2, we give the N-representability conditions fulfilled by the reconstructed 2-RDM for the 2-RDM-R$^{\mathrm{SDCI}}$ and the 2-RDM-R$^{\mathrm{FCI}}$ methods in the case of the neighbor excitation space for an interatomic distance of 2.5 Å since this is the only distance for which we can observe discrepancies between the two different excitation spaces.

The reconstructed 1-RDM does not seem to be affected by the change of the excitation space and fulfills in a good manner the N-representability condition checked since only seven eigenvalues are lower than the given threshold for the two excitation spaces.

The reconstructed 2-RDM fulfills very well the N-representability conditions for distances of 3.2 and 6.0 Å for both excitation spaces. But, for a distance of 2.5 Å, the quality of the reconstructed 2-RDM fails in the case of the 1 to 1 excitation space. When the neighbor excitation space is chosen (see Table 1), we observe a great difference compared to the 2-RDM-R$^{\mathrm{FCI}}$ method and find a total electronic energy larger than the FCI one. The major difference for the 2-RDM-R$^{\mathrm{SDCI}}$ method is related to the trace condition of the 2-RDM where the error decreases by one order of magnitude. Moreover, if we scan the reconstructed 2-RDM element by element, only one type of elements plays a role in the error related to the value of the trace of the 2-RDM. These elements are of the type ${}^{2}\Gamma^{i\sigma,r\sigma'}_{i\sigma,r\sigma}$ where i and r are, respectively, occupied and virtual orbitals of the same or different fragments.

In Table 3, the comparison between the values of these elements according to the excitation space considered (1 to 1 excitation space and neighbor excitation space) are presented for an interatomic distance of 2.5 Å. The values given are averaged values because for two atoms A and B, the elements ${}^{2}\Gamma^{i\sigma,r\sigma'}_{i\sigma,r\sigma}$ where i belong to A and r belong to B are of the same order. The shorter the distance between two atoms of Helium, the larger is the error without using the neighbor excitation space. At large distances or even at equilibrium length, the configurations added in SDCI calculations for the neighbor excitation space case do not play a crucial role and can be neglected for the calculation of the 2-RDM. Moreover, we can expect that for larger basis sets, the difference between the 1 to 1 excitation space and the neighbour excitation space would increase.

3.3 Applications to larger systems

3.3.1 *Results for He$_6$ in a larger basis set*

The linear chain He$_6$ has been considered with a larger basis set (ANO-l, 4s3p2d). The results obtained are summarized in Table 4. These calculations have been done to confirm the necessity of the use of neighbor excitation space and of type II fragments to obtain the dispersion energy with good accuracy. Indeed, the present system is known to show a very shallow energy minimum and represents a hard test for the 2-RDM-R method.

In Table 4, we have presented the energy differences between the reference taken at the CCSD(T) level and the SC**2 method or the 2-RDM-R$^{\mathrm{SDCI}}$ with the neighbor excitation space consideration and the "antisymmetrized product" with a cut-off radius of 5 Å.

Table 3 Comparison between the values according to the excitation space considered

n_{atom}	1–1 Excitation space	Neighbor excitation space
0	2.969 E − 05	1.70 E − 06
1	9.038 E − 05	1.94 E − 06
2	9.056 E − 05	3.87 E − 06
3	9.059 E − 05	3.95 E − 06

Table 4 Results for He$_6$ in a larger basis set

r	2.5	2.6	2.8	3.0	3.2	3.4	3.6	3.8	4.0	4.5	5.0	6.0	depth
He$_6$													6.67 E − 5
2-RDM-R$^{\mathrm{SDCI}}$	0.013040	0.013629	0.013610	0.013202	0.013147	0.013069	0.013094	0.013099	0.013109	0.013098	0.013125	0.013111	+10.87%
SC**2	0.009238	0.009087	0.008128	0.008043	0.008028	0.008042	0.008044	0.008040	0.008038	0.008057	0.008021	0.008059	+6.21%
d	2.5	2.8	3.2	3.4	3.6	3.8	4.0	4.5	5.0	6.0	7.0	7.5	depth
He$_4$													1.48 E $^{-4}$
2-RDM-R$^{\mathrm{SDCI}}$	4.623 E − 3	4.913 E − 3	4.924 E − 3	4.938 E − 3	4.920 E − 3	4.903 E − 3	4.890 E − 3	4.871 E − 3	4.862 E − 3	4.856 E − 3	4.854 E − 3	4.853 E − 3	+8.78%
MF	0.157252	0.156883	0.156622	0.156550	0.156517	0.156488	0.156468	0.156441	0.156429	0.156420	0.156418	0.156417	none

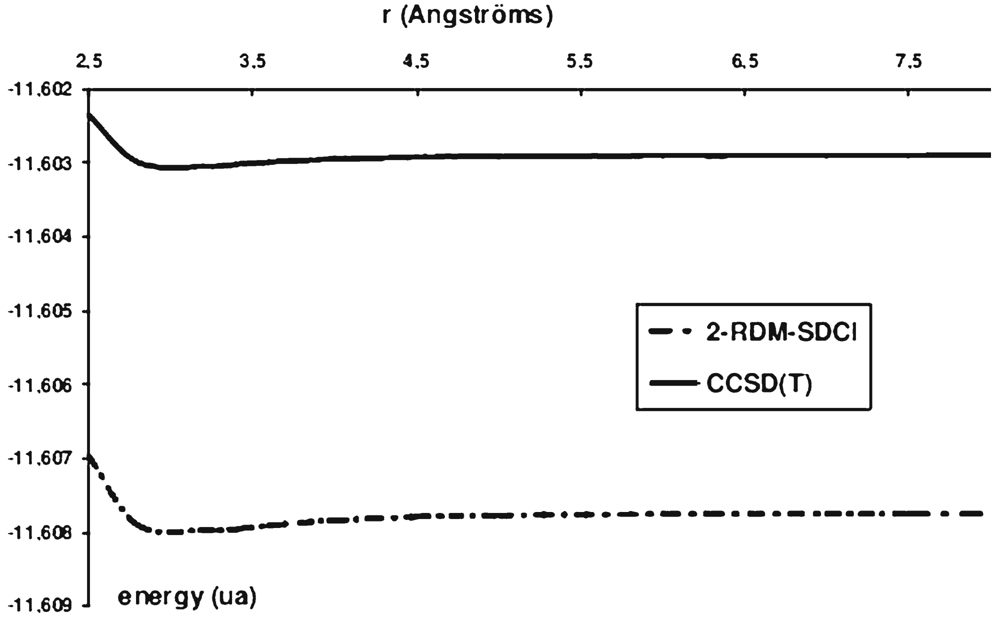

Fig. 5 Energy (ua) of the cluster of He^4 (ANO-l 4s3p2d) obtained by the CCSD(T) and 2-RDM-R^{SDCI} methods

In this case, we obtain a bond length shorter by 0.1 Å to the CCSD(T) one (3.2 Å) and a potential depth 10% larger than the CCSD(T) one. The SC**2 method gives very good results with an error of 6.12% only in comparison to the CCSD(T) results.

However, all along the curve there is a constant shift between the CCSD(T) solution and the 2-RDM-R^{SDCI} calculation. The 2-RDM-R^{SDCI} solution is lower than the CCSD(T) solution and proves that the N-representability conditions are not fulfilled in a good manner. This fact confirms the theoretical arguments given in Sect. 2.3 and the need for a control of the diexcitations done on each fragment.

3.3.2 Results for the cluster of He_4

We have considered the same basis set of orbitals for the He_4 cluster (ANO-l, 4s3p2d). Although this basis set is not large enough for an accurate description of this Helium cluster's properties, our purpose here is to compare the results obtained with the CCSD(T) ones. Moreover, with the neighbor excitation space, the whole virtual orbitals set has to be considered for each fragment calculation. Thus, the 2-RDM-R^{SDCI} method does not present a good computational cost for this example. Nevertheless, in the case of larger clusters, the computational would tend to grow linearly with the system size.

We have represented in Table 4 the energy differences obtained for He_4 for the CCSD(T) taken as reference, and the 2-RDM-R^{SDCI} and the HF methods. The computational cost of the SC**2 method was too high for this example. We can observe again that the 2-RDM-R^{SDCI} is lower than the CCSD(T) one but this difference is a constant shift and does not affect the accuracy of the potential depth. Concerning the accuracy of the 2-RDM-R^{SDCI} calculation, we obtain the depth of the potential energy with an order of 1.5×10^{-5} hartrees compared to the CCSD(T) solution (1.48×10^{-4} hartrees). The bond length is found to be 3.2 Å for the 2-RDM-R^{SDCI}. The results are better for the cluster because the excitation domains considered for each occupied orbital take into account the whole set of virtual orbitals. For a better understanding of the results, we have plotted in Fig. 5 the potential curves obtained for the CCSD(T) and 2-RDM-R^{SDCI} methods.

3.4 Conclusion

It has been shown that the proposed formalism could be suitable for the study of dispersion energy effects in weakly correlated systems. Indeed, the potential wells in the Van der Waals energy curves of Helium clusters are reproduced with a good accuracy, despite the smallness of the effects. The geometrical structures are also well reproduced with the 2-RDM-$R^{SD\text{-}CI}$ method. Moreover, this approach allows one to reduce the size-consistency error of a conventional SD-CI calculation on the whole system, this level of calculation being impossible due to its computational cost for the cluster considered. It has also been shown that in order to obtain accurate results, it is necessary to consider an excitation domain extended to virtual orbitals that do not belong to the fragment of the considered occupied orbitals.

The method has to be improved concerning the N- representability of the reconstructed 2-RDM by taking account of forbidden diexcitations, when successive configuration excitations on each fragment are considered. More work in this direction is needed in order to apply the 2-RDM-R method to larger clusters, where the N-representability problem could deteriorate the quality of the results.

Acknowledgements We would like to thank Mr J.-L. Heully and J.-P. Malrieu for their theoretical collaborations and useful discussions.

References

1. Ventknathan A, Szilva AB, Walter D, Gdanitz RJ, Carter EA (2004) J Chem Phys 120:1693
2. Hetzer G, Pulay P, Werner H-J (1998) Chem Phys Lett 290:143
3. Kinoshita T, Hino O, Bartlett RJ (2003) J Chem Phys 119:7756
4. Li S, Ma J, Jiang Y (2002) J Comput Chem 23:247
5. Scuseria GE, Ayala P (1999) J Chem Phys 111:8330
6. Schütz M, Werner H-J (2001) J Chem Phys 114:661
7. Walter D, Venkatnathan A, Carter EA (2003) J Chem Phys 118:8127
8. Martinez TJ, Carter EA (1995) J Chem Phys 102:7564
9. Janesko BG, Yaron D (2003) J Chem Phys 119:1320
10. Bories B, Evangelisti S, Leininger T, Maynau D (2004) Chem Phys Lett 385:225
11. Herbert JM, Harriman JE (2002) Phys Rev A 65:22511
12. Kutzelnigg W, Mukkherjee D (1999) J Chem Phys 110:2800
13. Coleman AJ, Yukalov VI (2000) Reduced density matrices Coulson's Challenge. Lecture notes in chemistry, vol 72. Springer, Berlin Heidelberg New York
14. Widmark P-O, Malmqvist P-A, Roos BO (1990) Theor Chim Acta 77:291
15. Garrod C, Percus JK (1964) J Math Phys 5:1756
16. Valdemoro C (1999) Electron correlation and reduced density matrices. Topics in Current Chemistry, 203. Springer, Berlin Heidelberg New York
17. Weinhold F, Bright Wilson EJ (1967) J Math Phys 47
18. Coleman AJ (1963) Rev Mod Phys 35:668
19. Cohen L, Frishberg C (1976) Phys Rev A 13:927
20. Valdemoro C, Tel LM, Pérez-Romero E (2000) Phys Rev A 61:32507
21. Mazziotti DA (2002) Phys Rev A 66:62503
22. Nakata M, Ehara M, Nakatsuji H (2002) J Chem Phys 116:5432
23. Mazziotti DA, Erdahl RM (2001) Phys Rev A 63:42113
24. Mazziotti DA (2002) Phys Rev A 65:62511
25. Nakata M, Ehara M, Yasuda K, Nakatsuji H (2000) J Chem Phys 12:8772
26. Kutzelnigg W (2003) Int J Quant Chem 95:404
27. Kutzelnigg W, Mukkherjee D (2000) Chem Phys Lett 317:567
28. Mukkherjee D, Kutzelnigg W (2001) J Chem Phys 114:2047
29. Mukkherjee D, Kutzelnigg W (2002) J Chem Phys 116:4787
30. Kutzelnigg W, Mukherjee D (1997) J Chem Phys 107:432
31. Jedrzejewskii J, Krokhmalskii T (2004) Phys Rev B 70:153102
32. Kohn W (1996) Phys Rev Lett 76:3168
33. Kaplan IG, Roszak S, Leszczynski J (2000) J Chem Phys 113:6245
34. Lindgren I, Morrison J (1982) Atomic many-body theory. Springer, Berlin Heidelberg New York
35. Maynau D, Evangelisti S, Guilhéry N, Calzado CJ, Malrieu J-P (2002) J Chem Phys 116:10060
36. Ben Amor N, Maynau D (1998) Chem Phys Lett 286:211
37. Heully J-L, Malrieu J-P (1992) Chem Phys Lett 192:135
38. Sebastianelli F, Di Paola C, Baccarelli I, Gianturco FA (2003) J Chem Phys 119:8276
39. Kàllay M, Surjàn PR (1999) Chem Phys Lett 312:221
40. Meissner L (1998) Chem Phys Lett 146:204
41. Lee MS, Maslen PE, Head-Gordon M (2000) J Chem Phys 112:3592